Pharmaceutical Research, Vol. 22, No. 3, March 2005 (© 2005)
DOI: 10.1007/s11095-004-1871-1

Research Paper

Intravenous Hydrophobic Drug Delivery: A Porous Particle Formulation of Paclitaxel (AI-850)

Julie A. Straub,[1,3] Donald E. Chickering,[1] Jonathan C. Lovely,[1] Huimin Zhang,[1] Bhavdeep Shah,[1] William R. Waud,[2] and Howard Bernstein[1]

Received September 28, 2004; accepted December 13, 2004

Purpose. To develop a rapidly dissolving porous particle formulation of paclitaxel without Cremophor EL that is appropriate for quick intravenous administration.
Methods. A rapidly dissolving porous particle formulation of paclitaxel (AI-850) was created using spray drying. AI-850 was compared to Taxol following intravenous administration in a rat pharmacokinetic study, a rat tissue distribution study, and a human xenograft mammary tumor (MDA-MB-435) model in nude mice.
Results. The volume of distribution and clearance for paclitaxel following intravenous bolus administration of AI-850 were 7-fold and 4-fold greater, respectively, than following intravenous bolus administration of Taxol. There were no significant differences between AI-850 and Taxol in tissue concentrations and tissue area under the curve (AUC) for the tissues examined. Nude mice implanted with mammary tumors showed improved tolerance of AI-850, enabling higher administrable does of paclitaxel, which resulted in improved efficacy as compared to Taxol administered at its maximum tolerated dose (MTD).
Conclusions. The pharmacokinetic data indicate that paclitaxel in AI-850 has more rapid partitioning from the bloodstream into the tissue compartments than paclitaxel in Taxol. AI-850, administered as an intravenous injection, has been shown to have improved tolerance in rats and mice and improved efficacy in a tumor model in mice when compared to Taxol.

KEY WORDS: drug delivery; hydrophobic drugs; microparticles; paclitaxel; spray drying.

INTRODUCTION

The poor aqueous solubility of hydrophobic drugs is a challenging formulation problem, particularly for intravenous delivery (1). It is estimated that 40% of new chemical entities have poor aqueous solubility (2). Poor aqueous solubility is, in particular, a common property of compounds identified using combinatorial chemistry and high-throughput screening (3). Thus, creating intravenous formulations of such compounds is of significant value. Paclitaxel, the active ingredient in the commercially available anticancer agent Taxol (paclitaxel injection, Bristol-Myers Squibb Oncology, Princeton, NJ, USA), has low aqueous solubility (4). Taxol consists of paclitaxel dissolved in Cremophor EL (BASF, Ludwigshafen, Germany; polyoxyethylated castor oil) and ethanol. Side effects observed with the intravenous administration of Taxol such as hypersensitivity reactions, nephrotoxicity, and neurotoxicity have been attributed to Cremophor (5). Due to such reactions, patients must be premedicated with corticosteroids and antihistamines, and Taxol must be administered as a 1–24 h infusion (6–7). Taxol is an important treatment of breast, ovarian, and non-small cell lung carcinomas (8–9), and modified formulations of paclitaxel that do not contain Cremophor are currently of significant interest (10–12). A number of nanoparticle- and microparticle-based formulations of paclitaxel, and related formulations such as liposomes and emulsions, have been reported in the literature (13–21). In these formulations, the paclitaxel is encapsulated within another material such as a hydrophobic polymer like poly (lactide *co*-glycolide) (PLGA), a protein, or lipids. These types of materials create a sustained-release system for paclitaxel with drug release occurring over hours to months. The porous particle formulation of paclitaxel (AI-850) discussed in this paper was developed with the goal of creating a rapidly dissolving formulation that could be administered as an i.v. bolus or a short infusion.

Acusphere's hydrophobic drug delivery system (HDDS), consisting of sub-micrometer to micrometer size porous particles, can be used to create rapidly dissolving formulations of hydrophobic drugs (22–25). The porous particles consist of drug microparticles and sub-micrometer particles and a water-soluble excipient such as a sugar or amino acid. During reconstitution, the water-soluble excipient dissolves, leaving a suspension of drug microparticles and sub-micrometer particles that dissolve upon further dilution in the plasma. The porous nature of the particles facilitates wetting and rapid dissolution of the encapsulated drug.

The production of the porous particles involves spray drying a solution containing the drug, the water-soluble excipient, and a pore-forming agent (i.e., a volatile salt). The

[1] TAcusphere, Inc., Watertown, Massachusetts 02472, USA.
[2] Southern Research Institute, Birmingham, Alabama 35205, USA.
[3] To whom correspondence should be addressed. (e-mail: julie.straub@acusphere.com)

pore-forming agent is volatilized along with the process solvent during the spray drying to produce a porous matrix comprising drug microparticles and the excipient. The water-soluble excipient facilitates wetting of the drug particles during reconstitution, provides proper osmolality to the dosage form, and improves the storage stability of the dry powder. The spray-drying process can be performed aseptically, and the resulting particles are in the appropriate size range for i.v. administration following reconstitution, as well as appropriate for administration by other parenteral routes, oral administration, and pulmonary administration.

This paper discusses the application of the hydrophobic drug delivery system to a rapidly dissolving formulation of paclitaxel for intravenous administration as an i.v. bolus or a short infusion and which would not require premedication of the patients with corticosteroids and antihistamines.

MATERIALS AND METHODS

Production of Microparticles

A paclitaxel-containing solution was prepared by dissolving paclitaxel (6.25 mg/ml), polysorbate 80 (0.625 mg/ml), and polyvinylpyrrolidone C15 (0.625 mg/ml) in ethanol. An aqueous solution was prepared containing the pore-forming agent (22), ammonium bicarbonate, at 2.5 mg/ml, and mannitol at 25 mg/ml. The aqueous solution was added to the ethanol solution in a ratio of 1:4. The resulting solution was spray dried on a spray dryer custom-designed to operate aseptically. The spray dryer was made from 316 stainless steel components with tri-clamp connections. The system was run under positive pressure with sterile-filtered nitrogen gas for the drying gas and atomization gas. A 0.22-μm filter was installed on the exhaust to maintain sterility and to capture any paclitaxel particulates that escape the spray-dryer cyclone.

The spray dryer used an internal mixing air-atomizing nozzle (the internal diameter of the fluid cap was 0.028″, and the internal diameter of the air cap was 0.060″) and nitrogen as the drying gas. Spray-drying conditions were as follows: 75 ml/min solution flow rate, 154 L/min atomization gas rate, 120 kg/h drying gas rate, 116°C inlet temperature, and 62°C outlet temperature. The resulting powder was collected, filled into glass vials, and stored at 2–8°C.

Paclitaxel Potency and Purity Analysis

For potency and purity analysis, AI-850 was dissolved in methanol:water:acetic acid (85:15:1) and analyzed by HPLC using an Agilent 1100 Series high pressure liquid chromotography (HPLC) (Agilent Technologies Inc., Palo Alto, CA, USA). Chromatographic conditions used for the analysis of paclitaxel used UV detection at 230 nm and a Phenomenex Curosil PFP column (5 μm, 250 × 4.6 mm) held at 35°C during analysis. The mobile phases used were A (acetonitrile:water, 35:65) and B (acetonitrile:water, 75:25), with a gradient running from 100% A to 85% A over 12 min, followed by a gradient running from 85% A to 0% A over the next 11.5 min. A flow rate of 1.5 ml/min was used. Potency values were obtained via comparison to a reference standard obtained from Hauser Laboratories (Boulder, CO, USA) and are based on 100% potency being the theoretical loading of the AI-850 powder based on the composition spray dried.

Differential Scanning Calorimetry (DSC)

DSC analyses were carried out on a TA 2920 differential scanning calorimeter (TA Instruments, New Castle, DE, USA) using nitrogen as the purge gas. Indium metal was used as the calibration standard. The samples were heated on the DSC at a heating rate of 10°C/min to a final temperature of 350°C.

Dry Powder Particle Size Analysis

Particle size analysis of AI-850 powder (prior to reconstitution) was performed using a Malvern Mastersizer (Malvern Instruments Ltd., Worcester, England) fitted with a dry powder module at a pressure of 65 psi.

Particle Size Analysis Post-Reconstitution

Particle size analysis of paclitaxel particles in AI-850 post-reconstitution was performed using a Multisizer II (Beckman Coulter Inc., Fullerton, CA, USA) equipped with a 50-μm aperture. The electrolyte used for the analysis contained sodium chloride (9 mg/ml), monobasic sodium phosphate monohydrate (0.19 mg/ml), anhydrous dibasic sodium phosphate (1.95 mg/ml), mannitol (55 mg/ml), polyvinylpyrollidone K15 (5.5 mg/ml), and was adjusted to pH 7.4 with 0.1 N HCl. The electrolyte solution was presaturated with paclitaxel immediately prior to use by addition of a solution of paclitaxel in methanol (35 mg paclitaxel/ml methanol; 4 ml to 1 L of modified electrolyte), followed by filtration through an 0.22-μm cellulose acetate filter to remove excess (precipitated) paclitaxel. The electrolyte was saturated with paclitaxel to ensure the paclitaxel particles in AI-850 did not dissolve upon dilution into the electrolyte for analysis. The presence of mannitol and polyvinylpyrollidone K15 in the electrolyte was found to suppress crystallization of paclitaxel from the paclitaxel-saturated electrolyte. The paclitaxel-saturated electrolyte was analyzed by Coulter Multisizer analysis prior to use for analysis of AI-850 suspensions to ensure that no significant crystallization of paclitaxel had occurred in the electrolyte solution. Suspensions of AI-850 were added to the paclitaxel-saturated electrolyte for analysis.

Microscopy

For transmission electron microscopy (TEM), AI-850 powder was embedded in a LR White Resin, which was then cut into thin (100–120 nm) sections on a diamond knife, and the sections were imaged on a Zeiss EM-10 transmission electron microscope (Zeiss Group, Jena, Germany) at 60 kV.

For scanning electron microscopy (SEM), the particles were sputter coated with platinum-palladium (80:20) and then imaged on a Hitachi S-4800 or a Hitachi S-2700 (Hitachi High Technologies America, Inc., San Jose, CA, USA).

For scanning electron microscopy (SEM) of paclitaxel particles post-reconstitution, the suspension post-reconstitution was filtered using an 0.22-μm filter, and the paclitaxel particles retained on the filter were rinsed with water and vacuum dried prior to sputter coating.

In Vitro Dissolution Analysis

Dissolution studies were conducted in PBS containing 0.08% Tween 80 (T80/PBS). T80/PBS (10 ml) was added to

an appropriate amount of material being tested to contain 5 mg of paclitaxel in a 15 ml polypropylene conical tube, and the suspension was vortexed to create a suspension of microparticles of paclitaxel. The suspension (0.25 ml) was then added to 250 ml of T80/PBS in a 600 ml glass beaker for dissolution analysis. Samples (1–2 ml) were removed and immediately filtered at each time-point. HPLC analysis was performed directly on the filtered aqueous solutions using an Agilent 1100 Series HPLC (Agilent Technologies Inc.). Chromatographic conditions used for the analysis of dissolution of paclitaxel used a Nucleosil column (5 μm, C18, 100A, 250 × 4.6 mm), a mobile phase of 2 mM H_3PO_4/acetonitrile (2:3) at a flow rate of 1.5 ml/min, UV detection at 227 nm, and a run time of 25 min. The concentration of paclitaxel in the dissolution media was 0.5 μg/ml. The saturation concentration observed for paclitaxel in T80/PBS was observed to be 1.5 μg/ml, and thus the dissolution assay was performed at a concentration lower than the saturation concentration of paclitaxel in the dissolution media.

Animal Care

In the three animal studies described below, cage size and animal care conformed to the guidelines of the *Guide for the Care and Use of Laboratory Animals,* 7th Edition (National Research Council, National Academy Press, Washington, DC, 1996), and the U.S. Department of Agriculture through the Animal Welfare Act (Public Law 99-198).

Pharmacokinetic Study of Paclitaxel in Rats

Male and female Sprague-Dawley rats (3/sex per group; animals were 8–11 weeks of age) were assigned to one of eight groups. Two groups received an i.v. bolus of Taxol (5 mg/kg or 10 mg/kg). Two groups received a 3 h i.v. infusion of Taxol (5 mg/kg or 10 mg/kg of paclitaxel). Four groups received an i.v. bolus of AI-850 (5 mg/kg, 10 mg/kg, 20 mg/kg, or 30 mg/kg of paclitaxel). AI-850 was reconstituted with water and diluted with D5W for dosing at a paclitaxel concentration of 10 mg/ml. Taxol was diluted with sterile saline for dosing at a paclitaxel concentration of 1 mg/ml.

Serial blood samples (0.3 ml) were taken during 24 h and processed into plasma. For the bolus dose groups, blood samples were collected at 0 min (pre-dose), 5 and 30 min, and at 1, 2, 3, 5, 8, 12, and 24 h after dosing. For the infusion groups, blood samples were collected at 0 min (pre-infusion) and at the following time-points after the start of the infusion: 30 min, and at 1, 2, 3, 4, 5, 8, 12, and 24 h. The plasma samples were analyzed for paclitaxel using a validated liquid chromatography/mass spectrometry/mass spectrometry (LC/MS/MS) assay at Southern Research Institute. The pharmacokinetic parameters were calculated assuming a two-compartment analysis using WinNonlin software.

Tissue Distribution Study of Paclitaxel in Rats

Single doses of either AI-850 or Taxol were administered intravenously via tail vein to groups of 18 male Sprague-Dawley rats/group. Animals were 8–9 weeks of age. The paclitaxel dose was 5.7 mg/kg for both formulations. AI-850 was reconstituted with water and diluted into D5W to a paclitaxel concentration of 6.9 mg/ml for administration. Taxol Injection was diluted with saline to a final paclitaxel concentration of 1.0 mg/ml for administration. Samples of plasma and selected tissues were collected from three rats/group at 0.5, 1, 2, 5, 12, and 24 h post-dose. The following tissues were collected and flash-frozen in liquid nitrogen: adrenal glands, brain, bone marrow, heart, kidney, liver, lung, muscle (back), small intestine (duodenum), sciatic nerve, spleen, testes, and thymus. Plasma and tissue samples were analyzed for concentrations of paclitaxel using a validated LC/MS/MS method (tissue samples were homogenized prior to analysis) at Southern Research Institute. Mean tissue paclitaxel concentration data were subjected to pharmacokinetic analyses using WinNonlin software. Values of AUC (area under the curve) were calculated using the trapezoidal rule. Plasma paclitaxel concentration data were fit to a compartmental model.

In Vivo Antitumor Efficacy Study in Mice

Mice were young (approximately 23 g), adult, female athymic NCr-Nu (14 mice/group). Mice were implanted subcutaneously with 30–40 mg fragments of the human mammary tumor MDA-MB-435 on day 0 (26). Treatment was scheduled to begin when the tumors ranged in size from 75 to 150 mg. Three groups were treated with AI-850 (15 mg/kg, 30 mg/kg, or 40 mg/kg of paclitaxel), one group was treated with the maximum tolerated dose (MTD) of Taxol (27) in this model (15 mg/kg of paclitaxel), and one control group was treated with D5W. AI-850 was reconstituted with 5% dextrose (D5W) to paclitaxel concentrations of 1.5 mg/ml, 3 mg/ml, and 4 mg/ml. Taxol was diluted with saline to a paclitaxel concentration of 1.5 mg/ml. Agents were administered via i.v. injection into the tail vein, once a day for 5 days. Mice were observed for survival, tumor size, and body weight. Tumors were measured by caliper in two dimensions and converted to tumor mass using the formula for a prolate elipsoid ($l \times w^2/2$).

Antitumor activity was assessed by the delay in tumor growth of the treated groups in comparison to the vehicle-treated control. The values for the time required for two tumor mass doublings (four times the original size) and t-c were calculated. The value of t-c (days) is the difference in the median of times post-implant for tumors of the treated groups to attain an evaluation size compared to the median of the control group. The time required for tumor mass doubling is calculated based on the initial tumor weight at the beginning of the treatment period, and values between measurements are calculated by exponential extrapolation.

RESULTS

Analysis of Paclitaxel Within AI-850

AI-850 was made via spray drying an ethanol-water solution containing paclitaxel, ammonium bicarbonate (the pore-forming agent), mannitol, polysorbate 80, and polyvinylpyrrolidone C15. As expected for a spray-drying process, paclitaxel encapsulation efficiency was essentially 100%, with observed values of chromatographic potency of 99.8% ± 1.5% (n = 6 lots). The chromatographic purity of paclitaxel in AI-850 was comparable to the purity of the starting bulk paclitaxel, indicating that the paclitaxel molecule was stable to the processing conditions. For example, the chromatographic purity of the paclitaxel for both the starting raw material and the lot of AI-850 used in the tissue distribution study were observed to be 99.5%. DSC analysis indicated that the paclitaxel within AI-850 was amorphous.

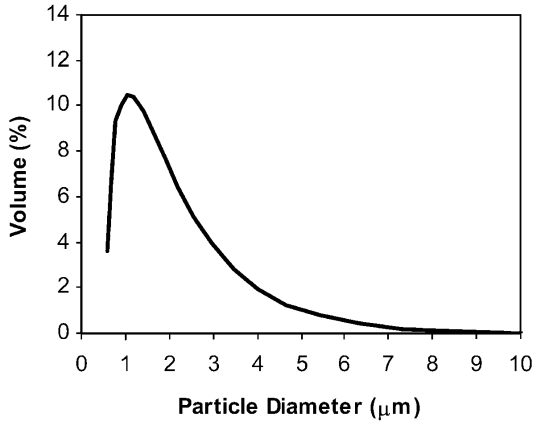

Fig. 1. Dry powder particle size distribution of AI-850 as analyzed on the Malvern Mastersizer.

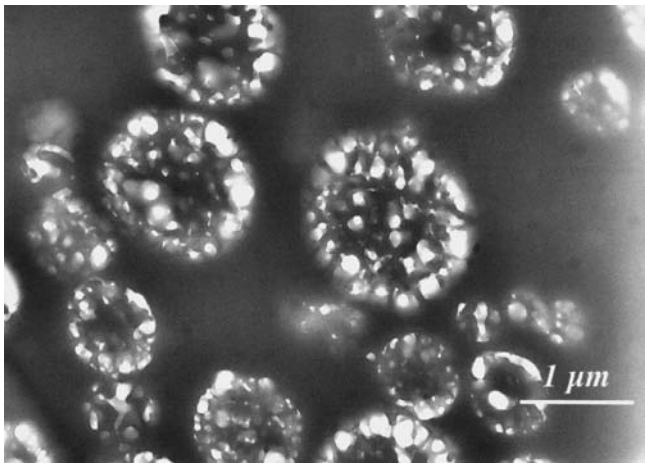

Fig. 3. TEM of cross section of AI-850 dry powder particles.

Particle Characteristics

The mean particle size for AI-850 prior to reconstitution was 1.53 μm ± 0.07 μm (n = 6 lots). A dry powder particle size distribution from a representative lot is shown in Fig. 1. The volume mean diameter is 1.52 μm, and 40% of the volume is less than 1.0 μm. A scanning electron micrograph of AI-850 particles is shown in Fig. 2, in which the surface of the microparticles appears relatively smooth, and the microparticles appear to be sphere-shaped. A transmission electron micrograph of cross-sections of AI-850 particles is shown in Fig. 3, where the bright white areas are the locations of the water-soluble excipients, the light gray areas are the locations of the paclitaxel, and the darker gray areas are the locations of the pores. Prior to reconstitution, the porosity of the AI-850 particles was predominantly internal.

Multiple analytical methods were evaluated as options for quantitative analysis of the particle size distribution of the paclitaxel particles within a reconstituted AI-850 suspension. Most of these methods (e.g., laser sizing methods) require large dilutions to obtain particle concentrations with the operating range of the respective detector, and as a result the AI-850–derived paclitaxel particles dissolved before analyses of such dilutions could be performed. A method for quantitative analysis was developed using a Coulter Multisizer II run using electrolyte saturated with paclitaxel, which prevents the rapid dissolution of the AI-850–derived paclitaxel particles. The particle size distribution of the paclitaxel particles from a reconstituted AI-850 suspension analyzed on a Coulter Multisizer is shown in Fig. 4, with an observed volume mean particle size of 2.0 μm. The Coulter Multisizer method used an aperture that could only detect particles down to 1 μm. Thus, unlike the Malvern Mastersizer analysis of the AI-850 microparticles, which had a lower limit of detection of 0.5 μm, the sub-micrometer particles were not detected with the Coulter Multisizer method, and the mean particle size value reported is an overestimation of the actual value. Attempts to perform suspension particle size analysis using a laser-based method on a Coulter LS230, which would have allowed for analysis of nano- and microparticles, using paclitaxel saturated media, were not successful due to problems attributed to the crystallization of paclitaxel within the paclitaxel-saturated media itself, affecting the LS230 analysis. An SEM image of paclitaxel particles isolated from a suspension post-reconstitution is shown in Fig. 5, which not only demonstrates the presence of microparticles of paclitaxel but also demonstrates that the microparticles themselves are internally porous, with significant surface porosity.

Paclitaxel dissolution for the parent bulk paclitaxel lot and for the average of 17 lots of AI-850 is shown in Fig. 6. These data illustrate that the process consistently produces a rapidly dissolving paclitaxel product.

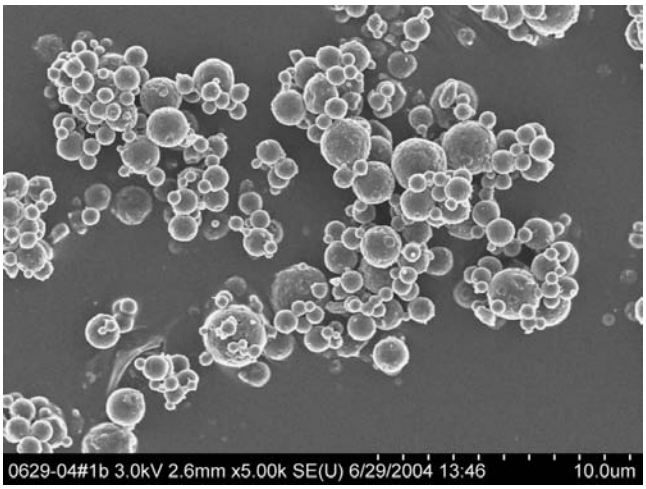

Fig. 2. SEM of AI-850 dry powder particles.

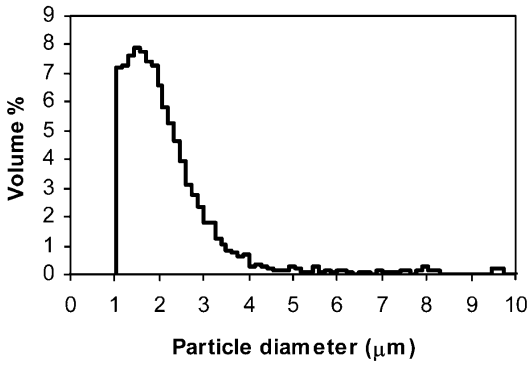

Fig. 4. Coulter Multisizer particle size distribution of reconstituted AI-850.

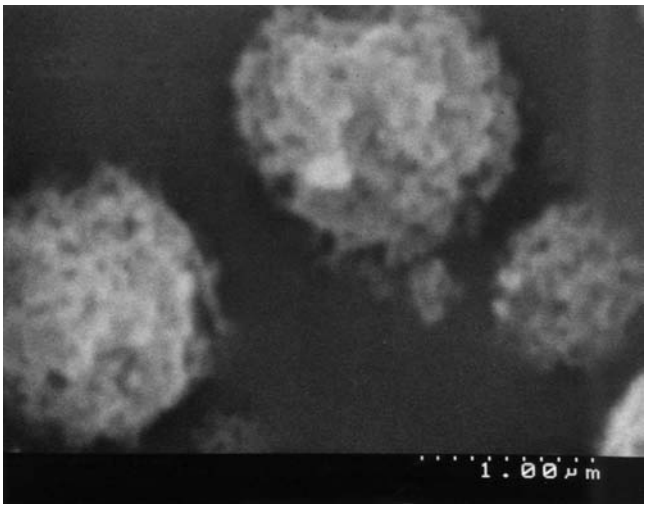

Fig. 5. SEM of AI-850 particles post-reconstitution.

Rat Pharmacokinetic Study

Plasma pharmacokinetic data for rats dosed with AI-850 and Taxol are shown in Fig. 7 and Table I. AI-850 was well tolerated at all doses (5 mg/kg, 10 mg/kg, 20 mg/kg, and 30 mg/kg of paclitaxel). Taxol administered as a 3-h infusion was also well tolerated at both dose levels (5 mg/kg and 10 mg/kg of paclitaxel). However, all the rats administered an i.v. bolus dose of Taxol at 10 mg/kg of paclitaxel died within 2 h.

Rat Tissue Distribution Study

Groups of rats were given an i.v. bolus dose of AI-850 (5.7 mg/kg of paclitaxel) or an i.v. bolus dose of Taxol (5.7 mg/kg of paclitaxel). Both an i.v. bolus dose of AI-850 (5.7 mg/kg of paclitaxel) and an i.v. bolus dose of Taxol (5.7 mg/kg of paclitaxel) were well tolerated. Data from selected time-points are shown in Table II, and tissue paclitaxel AUC values are shown in Table III.

In Vivo Antitumor Efficacy

To assess the efficacy of AI-850 in a tumor model, mice (young, adult female athymic NCr-Nu) were implanted subcutaneously (s.c.) with the human mammary tumor MDA-MB-435. Treatment began on day 14, when the median tumor size ranged from 108 to 144 mg (individual tumors ranging from 100 mg to 172 mg). The control tumors grew well, with a doubling time of approximately 10 days (200–400 mg). Agents were administered i.v. once a day for 5 days. Maximum weight losses observed were 4% for 15 mg/kg Taxol, and 0%, 9%, and 21% for AI-850 at 15 mg/kg, 30 mg/kg, and 40 mg/kg, respectively. Tumor weight data over time is shown in Fig. 8. At the 15 mg/kg dose, the time required for two tumor mass doublings was 59.6 days for Taxol and 56.9 days for AI-850, and the value of t-c was 44.4 days for Taxol and 41.7 days AI-850. For 30 mg/kg dose of AI-850, the time required for two tumor mass doublings was 66.4 days, and the value of

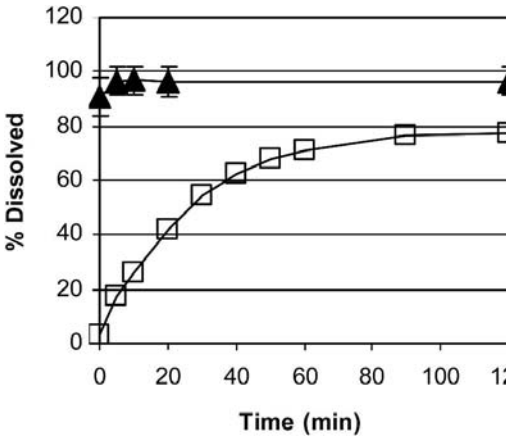

Fig. 6. *In vitro* dissolution of paclitaxel from bulk paclitaxel (□) and AI-850 (▲). For AI-850, the error bars represent the standard deviation for 17 lots.

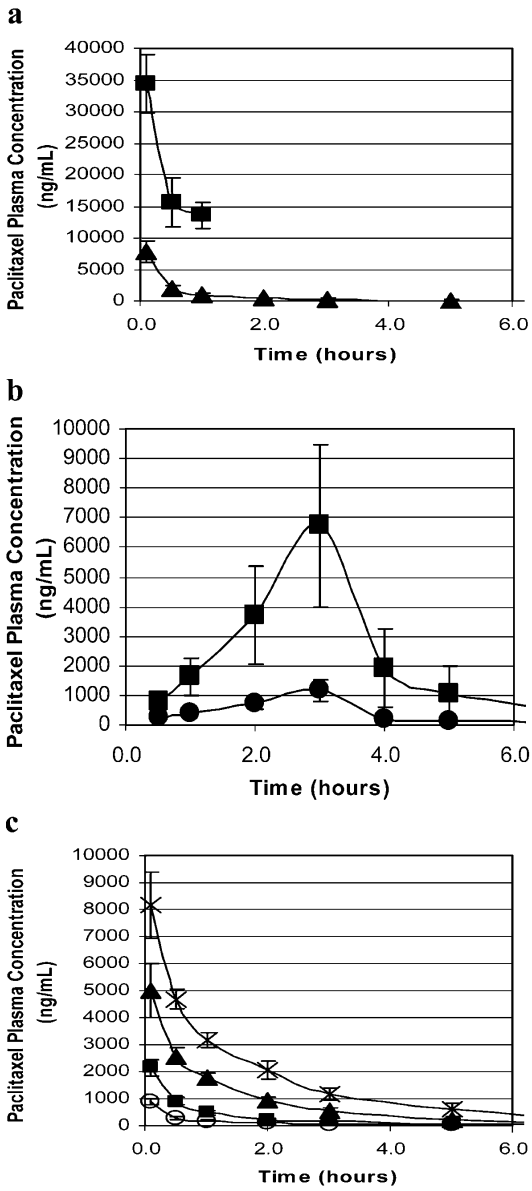

Fig. 7. Plasma paclitaxel concentrations in Sprague-Dawley rats. All values are means ± standard deviations for the combined data for male and female rats. (a) Treatment groups were Taxol Bolus at 5 mg/kg (▲) and 10 mg/kg (■). (b) Treatment groups were Taxol Infusion at 5 mg/kg (●) and 10 mg/kg (■). (c) Treatment groups were AI-850 Bolus at 5 mg//kg (○), 10 mg/kg (■), 20 mg/kg (▲), and 30 mg/kg (×).

Table I. Pharmacokinetic Analysis of Paclitaxel Formulations

PK parameter	Taxol i.v. bolus 5 mg/kg	Taxol i.v. bolus 10 mg/kg	Taxol 3-h infusion 5 mg/kg	Taxol 3-h infusion 10 mg/kg	AI-850 i.v. bolus 5 mg/kg	AI-850 i.v. bolus 10 mg/kg	AI-850 i.v. bolus 20 mg/kg	AI-850 i.v. bolus 30 mg/kg
AUC[a] (ng · h/ml)	4427 ± 994	NA[b]	2601 ± 386	12,670 ± 5741	854 ± 49	2095 ± 213	6524 ± 388	12,434 ± 1558
$T_{1/2\alpha}$ (h)	0.31 ± 0.09	NA[b]	0.53 ± 0.11	1.04 ± 0.25	0.24 ± 0.07	0.40 ± 0.12	0.77 ± 0.32	0.62 ± 0.34
$T_{1/2\beta}$ (h)	2.80 ± 0.25	NA[b]	5.98 ± 1.03	5.96 ± 0.83	3.49 ± 0.72	3.18 ± 0.56	3.28 ± 1.37	2.50 ± 0.68
C_l (ml h^{-1} kg^{-1})	1255 ± 256	NA[b]	2249 ± 306	761 ± 231	5309 ± 318	4388 ± 465	2460 ± 154	2070 ± 259
V_{dss} (ml/kg)	2289 ± 487	NA[b]	8363 ± 2063	2085 ± 617	17,011 ± 2458	10,847 ± 1860	5747 ± 1094	4778 ± 690
$C_{max\ measured}$ (ng/ml)	7742 ± 1763	35,338 ± 15,541	1170 ± 359	6725 ± 2745	912 ± 116	2140 ± 320	4980 ± 998	8162 ± 1210

[a] AUC for the 10 mg/kg 3-h infusion of Taxol was calculated over 0 to 24 h, whereas all the other AUC values were calculated over 0 to 12 h.
[b] These data are not available for the group receiving a 10 mg/kg i.v. bolus of Taxol, as the rats died shortly after dosing.
The values shown are the mean ± SD for combined data for male and female rats (n = 6).

t-c was 51.2 days. For 40 mg/kg dose of AI-850, the time required for two tumor mass doublings was >76 days, and the value of t-c was >61 days.

DISCUSSION

AI-850 is produced via spray drying a solution containing paclitaxel, mannitol, polyvinylpyrrolidone C15, polysorbate 80, and ammonium bicarbonate (the pore-forming agent). The pore-forming agent, ammonium bicarbonate, is removed during processing. Although spray drying has been described in the literature for a paclitaxel formulation, it has been for the production of a poly (lactic-*co*-glycolic acid)–based sustained-release microsphere formulation of paclitaxel (21), whereas AI-850 is an immediate-release formulation of paclitaxel.

The level of mannitol present in AI-850 is such that, post-reconstitution, AI-850 is iso-osmotic. The level of polysorbate 80 present in AI-850 (10% of the paclitaxel level) would result in a dose of 0.47 mg/kg polysorbate based on the standard dose of paclitaxel (175 mg/m^2; 4.7mg/kg), which is well below doses of polysorbate 80 in commercial intravenously administered products. For example, Taxotere (Aventis Pharmaceuticals, Inc., Bridgewater, NJ, USA), which is a similar chemotherapeutic to Taxol, is formulated with polysorbate 80. A standard dose of docetaxol from Taxotere (75 mg/m^2; 2 mg/kg) would contain 52 mg/kg of polysorbate 80.

Table II. Rat Tissue Distribution of Paclitaxel

Organ	Agent	Mean (±SD) paclitaxel concentration (ng/g or ng/ml)			
		0.5 h	2 h	5 h	12 h
Adrenal gland	AI-850	13,637 ± 2068	6048 ± 1439	3298 ± 493	1659 ± 214
	Taxol	17,455 ± 1391	6317 ± 455	4136 ± 1031	996 ± 23
Bone marrow	AI-850	2424[a]	2953[a]	2510[a]	1245[a]
	Taxol	3034[a]	3171[a]	2778[a]	1440[a]
Brain	AI-850	112 ± 18	101 ± 32	49 ± 11	36 ± 9
	Taxol	161 ± 18	75 ± 12	57 ± 12	BLOQ
Heart	AI-850	8897 ± 570	3767 ± 1060	1693 ± 226	710 ± 40
	Taxol	11,073 ± 2175	4604 ± 816	2499 ± 636	603 ± 10
Kidney	AI-850	14,123 ± 1086	6585 ± 1664	3113 ± 487	1414 ± 239
	Taxol	17,650 ± 1477	7820 ± 1147	4282 ± 1697	847 ± 25
Liver	AI-850	19,102 ± 3998	10,630 ± 5856	2887 ± 549	1757 ± 144
	Taxol	22,392 ± 5630	10,107 ± 2160	7701 ± 3470	2057 ± 547
Lung	AI-850	14,047 ± 11,160	9743 ± 5332	3839 ± 3344	1842 ± 390
	Taxol	11,467 ± 1396	5916 ± 1023	2895 ± 476	842 ± 86
Muscle	AI-850	2867 ± 411	2330 ± 426	1675 ± 149	1024 ± 87
	Taxol	3449 ± 341	3477 ± 323	2132 ± 154	905 ± 143
Plasma	AI-850	564 ± 14	185 ± 122	42 ± 5	18 ± 4
	Taxol	4780 ± 886	792 ± 149	343 ± 170	43 ± 5
Sciatic nerve	AI-850	1226 ± 333	802 ± 105	581 ± 61	345 ± 33
	Taxol	1860 ± 579	1787 ± 347	989 ± 306	311 ± 33
Small intestine	AI-850	11,323 ± 949	6270 ± 3107	3003 ± 709	1567 ± 63
	Taxol	14,698 ± 3536	8957 ± 2562	5008 ± 1087	1924 ± 182
Spleen	AI-850	11,385 ± 1644	6960 ± 826	4554 ± 811	2090 ± 86
	Taxol	13,392 ± 611	8757 ± 196	6174 ± 1252	1578 ± 217
Testes	AI-850	221 ± 27	285 ± 86	229 ± 47	181 ± 24
	Taxol	323 ± 65	243 ± 42	377 ± 61	237 ± 45
Thymus	AI-850	2245 ± 733	2288 ± 866	2106 ± 393	2560 ± 445
	Taxol	2552 ± 138	3477 ± 323	2132 ± 154	905 ± 143

[a] Sample from all animals was pooled at each time-point due to small tissue sample size.

Table III. Paclitaxel AUC in Rat Tissues

Organ	Agent	$AUC_{0\text{-}inf}$ (ng·h/ml)
Adrenal gland	AI-850	66,466
	Taxol	64,120
Bone marrow	AI-850	45,817
	Taxol	40,060
Brain	AI-850	1146
	Taxol	1167
Heart	AI-850	34,572
	Taxol	40,777
Kidney	AI-850	66,516
	Taxol	66,359
Liver	AI-850	80,642
	Taxol	107,218
Lung	AI-850	126,782
	Taxol	49,870
Muscle	AI-850	38,759
	Taxol	37,385
Plasma	AI-850	1409
	Taxol	7541
Sciatic nerve	AI-850	13,016
	Taxol	16,647
Small intestine	AI-850	67,659
	Taxol	85,043
Spleen	AI-850	86,871
	Taxol	84,820
Testes	AI-850	19,680
	Taxol	22,750
Thymus	AI-850	NA
	Taxol	1,432,935

Two key parameters for intravenously administered suspensions of drug particles are particle size and dissolution rate. The particle size of reconstituted AI-850 was shown to be appropriate for intravenous administration, with a volume mean suspension particle size of less than 2.0 μm. The TEM of sections of AI-850 particles and the SEM image of the paclitaxel particles demonstrate the porous nature of the particles.

Lot to lot reproducibility of rapid *in vitro* dissolution of paclitaxel in AI-850 was observed (Fig. 6). Paclitaxel in AI-850 dissolved *in vitro* significantly more rapidly than the parent bulk drug, with 95% of the paclitaxel in AI-850 dissolved in 5 min.

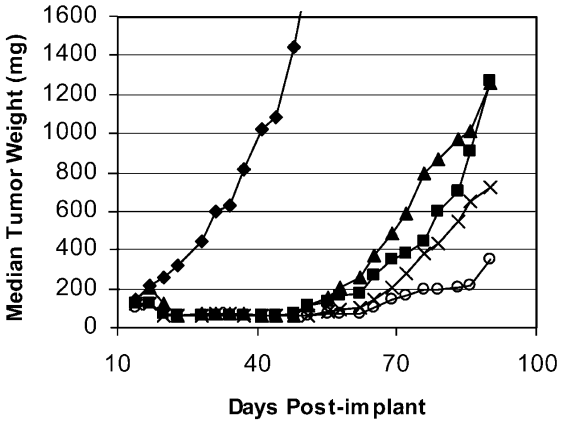

Fig. 8. Mouse MDA-MB-435 xenograft mammary tumor efficacy data (median tumor weight for n = 14) for the 5% dextrose control (♦), 15 mg/kg Taxol (■), 15 mg/kg AI-850 (▲), 30 mg/kg AI-850 (×), and 40 mg/kg AI-850 (○).

Following a single i.v. bolus dose of AI-850 ranging from 5 to 30 mg/kg of paclitaxel, plasma concentrations of paclitaxel increased with increasing dose (Fig. 7c). The increases in C_{max} were disproportionately greater than the increases in AI-850 doses, however, the ratio of mean measured C_{max} was never more than 2.5 for a 2-fold increase in dose (Table I). $AUC_{0\text{-}12}$ also increased disproportionately to dose. Both clearance (C_l) and steady-state volume of distribution (V_{dss}) decreased with increasing dose of AI-850, suggesting saturation of the elimination and/or distribution mechanism. Values for initial half-life ($t_{1/2\alpha}$) and terminal half-life ($t_{1/2\beta}$) were consistent across the AI-850 doses tested. Overall, no differences between the sexes were observed in the plasma pharmacokinetics of paclitaxel following i.v. bolus administration of AI-850.

For rats receiving Taxol at 5 or 10 mg/kg of paclitaxel by either i.v. bolus or 3-h infusion, plasma concentrations of paclitaxel increased more than proportionately with increasing dose (Fig. 7a,b). Doubling the i.v. bolus dose of Taxol from 5 to 10 mg/kg of paclitaxel resulted in a 4.5-fold increase in mean measured C_{max} at 5 min post-dose (Table I). Likewise, at the end of the 3-h infusion period in the 5 mg/kg and the 10 mg/kg paclitaxel groups, plasma concentrations of paclitaxel were 6-fold higher for animals receiving Taxol at 10 mg/kg of paclitaxel than for animals receiving Taxol at 5 mg/kg of paclitaxel. The C_l and V_{dss} of paclitaxel were lower in the 10 mg/kg Taxol infusion group as compared to the 5 mg/kg Taxol infusion group. Values for terminal half-life ($t_{1/2\beta}$) were longer when Taxol was administered as a 3-h infusion than when administered by i.v. bolus. This difference may be due to either true differences in pharmacokinetics with i.v. Taxol bolus *vs.* Taxol infusion dosing or an inability to determine a true terminal half-life within the limitations of the sampling times and the assay sensitivity. Overall, no differences between the sexes were observed in the plasma pharmacokinetics of paclitaxel following i.v. bolus or i.v. infusion administration of Taxol.

A comparison of the pharmacokinetic results for AI-850 and Taxol administered as i.v. bolus doses (Table I) demonstrates that at the 5 mg/kg dose, the C_l and Vd_{ss} of paclitaxel were 4- and 7-fold higher in those animals receiving AI-850 as compared to those receiving Taxol. Both $t_{1/2\alpha}$ and $t_{1/2\beta}$ were similar across all i.v. bolus dose groups of AI-850 and Taxol. The paclitaxel C_{max} achieved following i.v. bolus administration of Taxol 5 mg/kg was 8-fold higher than that achieved with i.v. bolus administration of the same dose of AI-850. The data indicate that paclitaxel in AI-850 partitions more rapidly from the bloodstream into the tissue compartments than the paclitaxel in Taxol.

Pharmacokinetic studies of Taxol in animals (28) and in man (29) have shown poor dose linearity. The deviation from linearity for Taxol has been ascribed to the presence of Cremophor EL in the Taxol formulation, which entraps paclitaxel within micelles (30). It has been reported that the pharmacokinetics of paclitaxel does not correlate with efficacy but does correlate with toxicity (28). Specifically, increased hematological toxicity appeared to correlate with increased plasma AUC (31) or with increased duration of time above a threshold plasma concentration level (32). However, the cause of the acute mortality observed for the i.v. bolus of

Taxol in this study was not investigated. For intravenous delivery of paclitaxel, the goal is not the direct delivery of the drug to the systemic circulation, but rather the distribution of the drug to the site of action (the tumor tissue). The Cremophor in Taxol artificially increases the circulating levels of paclitaxel (30). The paclitaxel delivered as AI-850 partitions into the tissue compartment more rapidly, which may have potential safety benefits.

The plasma pharmacokinetic results within the tissue distribution study were similar to those observed in the previously described pharmacokinetic study (Table I). After administration of either formulation, paclitaxel concentrations peaked at the first sampling time-point (0.5 h) in well-perfused organs such as the liver and kidney (Table II). The mean paclitaxel concentrations measured in most organs, including the liver, kidney, brain, and sciatic nerve, were similar at each time-point after administration of either Taxol or AI-850 (Table II), and the calculated values for tissue $AUC_{0-\infty}$ for Taxol and AI-850 were similar (Table III). Thus, the significant differences in the plasma concentrations induced by each formulation did not result in any significant differences in tissue concentrations over time. This finding is similar to literature findings for tissue distribution data for paclitaxel in mice after administration of multiple dose levels of paclitaxel in either dimethyl acetamide or Cremophor EL–ethanol (1:1) diluted into saline, where tissue AUC values were equivalent for paclitaxel in the two diluents and were close to linear, but the plasma profiles were significantly different (33–34).

In this tumor model study, both Taxol and AI-850 were tolerated. However, the highest dose of AI-850 (40 mg/kg) did elicit a maximum body weight loss of 21%, compared to 9% for 30 mg/kg of AI-850, 0% for 15 mg/kg of AI-850, and 4% for 15 mg/kg of Taxol. The tumor weight data are shown in Fig. 8. At equivalent doses (5 days × 15 mg/kg), Taxol and AI-850 had similar tumor response in the mouse model as assessed based on the value of the time required for two tumor mass doublings (59.6 days for Taxol vs. 56.9 days for AI-850) and on the value of t-c (44.4 days for Taxol vs. 41.7 days AI-850). It was possible to dose paclitaxel in the form of AI-850 at a higher paclitaxel dose than the MTD of paclitaxel in the form of Taxol (15 mg/kg). These higher doses of AI-850 resulted in prolonged tumor response as evidenced by a greater delay in the time to tumor regrowth (59.6 days for 15 mg/kg of Taxol vs. >76 days for 40 mg/kg of AI-850) and based on a larger value of t-c (44.4 days for 15 mg/kg of Taxol vs. >61 days for 40 mg/kg of AI-850). This study demonstrates the *in vivo* activity of AI-850 against the human MDA-MB-435 mammary tumor.

There have been other nano- and microparticle formulations of paclitaxel, or related formulations such as liposomes and emulsions, described in the literature (10–21), which generally function as sustained-release systems for paclitaxel, relative to the immediate release (rapid dissolution) of AI-850. The encapsulating materials of the other formulations and the size of the particles will also influence the disposition of the drug in the body, as intact particles are cleared from the bloodstream by the phagocytic cells of the reticuloendothelial system (35–39). In the case of AI-850, the particles are intended to dissolve rapidly in the bloodstream, and thus the clearance of paclitaxel will be governed by the normal disposition of the drug. Many of these formulations are targetting intravenous delivery, with a similar goal to that of AI-850, to provide a safer, Cremophor-free formulation. The success of such products is dependent upon a number of factors such as chemical and physical characteristics of the products, and the resulting efficacy and safety in humans, which can only be evaluated in a controlled clinical setting.

CONCLUSIONS

AI-850, a porous particle formulation of paclitaxel, was shown to have appropriate size and dissolution rate for intravenous administration. AI-850 did not contain Cremophor, and thus Cremophor-related reactions could potentially be avoided. The pharmacokinetics and tissue distribution of paclitaxel administered intravenously as AI-850 were assessed in a series of nonclinical studies. Studies in rats indicated that, when compared to similar paclitaxel doses administered as Taxol, C_{max} and AUC were generally lower for AI-850, wherease C_l and V_{dss} were greater for AI-850 than for Taxol, indicating that AI-850 has a more rapid partitioning of paclitaxel from the bloodstream into the tissue compartments. In contrast, the tissue concentrations of paclitaxel in rats were similar for the two formulations administered at the same dose level. The AI-850 formulation of paclitaxel appears to offer tissue distribution characteristics similar to those of Taxol, while potentially avoiding the high plasma concentrations and the toxicity associated with the latter formulation (28,31–32). Notably, AI-850 was found to be better tolerated as an i.v. bolus than Taxol.

In the human xenograft mammary tumor model in mice, comparable doses of AI-850 and Taxol produced comparable results. However, the MTD of AI-850 was higher than the MTD of Taxol, and thus doses of AI-850 could be administered that were higher than the MTD of Taxol. This increase in dose was associated with an increase in efficacy based on a greater delay in the time to tumor regrowth for AI-850 as compared to Taxol.

The data presented herein demonstrate that rapidly dissolving porous particles can be used for intravenous delivery of hydrophobic drugs such as paclitaxel. A Phase I clinical study of AI-850 was recently completed (40).

ACKNOWLEDGMENTS

The authors acknowledge Patricia Noker, James Johnson, Tsu-Han Lin, and Eric J. Morinello of Southern Research Institute, William Fowle of Northeastern University Center for Electron Microscopy, and Sarwat Khattak and Robert Zelle for their contributions to this work.

REFERENCES

1. S. N. Pace, G. W. Pace, I. Parikh, and A. K. Mishra. Novel injectable formulations of insoluble drugs. *Pharm. Technol.* **23**:116–134 (1999).
2. M. Hite, S. Turner, and C. Federici. Part 1: Oral delivery of poorly soluble drugs. *Pharm. Manuf. Packing Sourcer* **Autumn**: 38–40 (2003).
3. C. Lipinski. Poor aqueous solubility – an industry wide problem in drug discovery. *Am. Pharm. Rev.* **5**:82–85 (2002).
4. R. T. Liggins, W. L. Hunger, and H. M. Burt. Solid-state characterization of paclitaxel. *J. Pharm. Sci.* **86**:1458–1463 (1997).
5. L. van Zulen, J. Verweij, and A. Sparreboom. Role of formulation vehicles in taxane pharmacology. *Invest. New Drugs* **19**:125–141 (2001).

6. E. K. Rowinsky. The taxanes: dosing and scheduling considerations. *Oncology* **11**(Suppl.):7–19 (1997).
7. F. A. Greco and T. M. Hainsworth. One-hour paclitaxel infusions: a review of safety and efficacy. *Cancer J. Sci. Am.* **5**:179–191 (1999).
8. E. K. Rowinsky and R. C. Donehower. Paclitaxel (Taxol). *N. Engl. J. Med.* **332**:1004–1014 (1995).
9. E. K. Rowinsky. Paclitaxel pharmacology and other tumor types. *Semin. Oncol.* **24**:S19-1–S19-12 (1997).
10. A. K. Singla, A. Garg, and D. Aggarwal. Paclitaxel and its formulations. *Int. J. Pharm.* **235**:179–192 (2002).
11. S. Nuijen, M. Bouma, J. H. Schellens, and J. H. Beijnen. Progress in the development of alternative pharmaceutical formulations of taxanes. *Invest. New Drugs.* **19**:143–153 (2001).
12. R. Pawar, A. Shikanov, B. Vaisman, and A. J. Domb. Intravenous and regional paclitaxel formulations. *Curr. Med. Chem.* **11**: 397–402 (2004).
13. S. S. Feng, L. Mu, K. Y. Win, and G. Huang. Nanoparticles of biodegradable polymers for clinical administration of paclitaxel. *Curr. Med. Chem.* **11**:413–424 (2004).
14. N. K. Ibrahim, N. Desai, S. Legha, P. Soon-Shiong, R. L. Theriault, E. Rivera, B. Esmaeli, S. E. Ring, A. Bedikian, G. N. Hortobagyi, and J. A. Ellerhorst. Phase I and pharmacokinetic study of ABI-007, a Cremaphor-free, protein-stabilized, nanoparticle formulation of paclitaxel. *Clin. Cancer Res.* **8**:1038–1044 (2002).
15. T. Y. Kim, D. W. Kim, J. W. Chung, S. G. Shin, S. C. Kim, D. S. Heo, N. K. Kim, and Y. J. Bang. Phase I and pharmacokinetic study of Genexol-PM, a Cremophor-free, polymeric micelle-formulated paclitaxel, in patients with advanced malignancies. *Clin. Cancer Res.* **10**:3708–3716 (2004).
16. P. P. Constantinides, A. Tustian, and D. R. Kessler. Tocol emulsions for drug solubilization and parenteral delivery. *Adv. Drug Deliv. Rev.* **56**:1243–1255 (2004).
17. O. Soepenberg, A. Sparreboom, M. J. de Jonge, A. S. Planting, G. de Heus, W. J. Loos, C. M. Hartman, C. Bowden, and J. Verweij. Real-time pharmacokinetics guiding clinical decisions; phase I study of a weekly schedule of liposome encapsulated paclitaxel in patients with solid tumors. *Eur. J. Cancer* **40**:681–688 (2004).
18. S. Streith, M. E. Eichhorn, B. Sauer, B. Schulze, M. Teifel, U. Michaelis, and M. Dellian. Neovascular targeting chemotherapy: encapsulation of paclitaxel in cationic liposomes impairs functional tumor microvasculature. *Int. J. Cancer* **111**:117–124 (2004).
19. W. R. Perkins, I. Ahmad, X Li, D. J. Hirsh, G. R. Masters, C. J. Fecko, S. Ali, J. Nguyen, J. Schupsky, C. Herbert, A. S. Janoff, and E. Mayhew. Novel therapeutic non-particles (lipocores): trapping poorly water soluble compounds. *Int. J. Pharm.* **200**:27–39 (2001).
20. E. Harper, W. Dang, R. G. Lapidus, and R. I. Garver. Enhanced efficacy of a novel controlled release paclitaxel formulation (PACLIMER delivery system) for local-regional therapy of lung cancer tumor nodules in mice. *Clin. Cancer Res.* **5**:4242–4248 (1999).
21. L. Mu and S. S. Feng. Fabrication, characterization and in vitro release of paclitaxel (Taxol®) loaded poly (lactic-co-glycolic acid) microspheres prepared by spray drying technique with lipid/cholesterol emulsifiers. *J. Control. Rel.* **76**:239–254 (2001).
22. J. A. Straub, E. Mathiowitz, H. Bernstein, H. T. Brush, and R. E. Wing. Method for making porous microparticles by spray drying. Acusphere, Inc. U.S. Patent No. 5,853,698 (1998).
23. J. Straub, H. Bernstein, D. E. Chickering, S. Khattak, and G. Randall. Porous drug matrices and methods of manufacture thereof. Acusphere, Inc. U.S. Patent No. 6,395,300 (2002).
24. J. Straub, H. Bernstein, D. E. Chickering, S. Khattak, and G. Randall. Porous paclitaxel matrices and methods of manufacture thereof. Acusphere, Inc.. U.S. Patent No. 6,610,317 (2003).
25. J. Straub, H. Bernstein, D. E. Chickering, and G. Randall. Porous celecoxib matrices and methods of manufacture thereof. Acusphere, Inc. U.S. Patent No. 6,589,557 (2003).
26. J. Plowman, D. J. Dykes, M. Hollingshead, L. Simpson-Herren, and M. C. Alley. Human tumor xenograft models in NCI drug development. In B. A. Teicher (eds.), *Anticancer Drug Development Guide: Preclinical Screening, Clinical Trials, and Approval,* Humana Press, Totowa, NJ, 1997, pp. 101–125.
27. Data on file with Southern Research Institute, Birmingham, AL, USA.
28. C. M. Spenser and D. Faulds. Paclitaxel: a review of its pharmacodynamic and pharmacokinetic properties and therapeutic potential in the treatment of cancer. *Drugs* **48**:794–847 (1994).
29. C. M. Kearns. Pharmacokinetics of the taxanes. *Pharmacotherapy* **17**:105S–109S (1997).
30. L. van Zuylen, M. O. Karlsson, J. Verweij, E. Brouwer, P. de Bruijn, K. Nooter, G. Stoter, and A. Sparreboom. Pharmacokinetic modeling of paclitaxel encapsulation in Cremophor EL micelles. *Cancer Chemother. Pharmacol.* **47**:309–318 (2001).
31. A. Sparreboom and J. Verweij. Paclitaxel pharmacokinetics, threshold models and dosing strategies. *J. Clin. Oncol.* **21**:2804–2805 (2003).
32. L. Gianni, C. M. Kearns, G. Giani, G. Capri, L. Vigano, A. Lacatelli, G. Bonadonna, and M. J. Egorin. Nonlinear pharmacokinetics and metabolism of paclitaxel and its pharmacokinetic/pharmacodynamic relationships in humans. *J. Clin. Oncol.* **13**: 180–190 (1995).
33. A. Sparreboom, O. van Telligen, W. J. Nooijen, and J. H. Beijnen. Tissue distribution, metabolism and excretion of paclitaxel in mice. *Anticancer Drugs* **7**:78–86 (1996).
34. A. Sparreboom, O. van Telligen, W. J. Nooijen, and J. H. Beijnen. Nonlinear pharmacokinetics of paclitaxel in mice results from the pharmaceutical vehicle Cremophor EL. *Cancer Res.* **56**:2112–2115 (1996).
35. L. Brannon-Peppas and J. O. Blanchette. Nanoparticle and targeted systems for cancer therapy. *Adv. Drug Deliv. Rev.* **56**:1649–1659 (2004).
36. K. Ogawara, K. Higaki, and T. Kimura. Major determinants in hepatic disposition of polystyrene nanospheres: implication for rational design of particulate drug carriers. *Crit. Rev. Ther. Drug Carrier Syst.* **19**:277–306 (2002).
37. S. S. Davis and L. Illum. Polymeric microspheres as drug carriers. *Biomaterials* **9**:111–115 (1988).
38. N. Oku and Y. Namba. Long-circulating liposomes. *Crit. Rev. Ther. Drug Carrier Syst.* **11**:231–270 (1994).
39. T. Sakaeda and K. Hirano. Effect of composition on biological fate of oil particles after intravenous injection of o/w lipid emulsions. *J. Drug Target.* **6**:273–284 (1998).
40. A. J. Olsanski, L. D. Lewis, C. Mita, R. C. Walovitch, R. P. Perez, D. P. Tuck, and E. K. Rowinsky. Phase 1 and pharmacokinetic study of AI-850, a novel microparticle hydrophobic drug delivery system (HDDS) for paclitaxel. *J. Clin. Oncol.* **22**(Suppl.):2048 (2004).